Resonant second harmonic generation in ZnSe bulk microcavity

Vittorio Pellegrini, Raffaele Colombelli, Iacopo Carusotto, and Fabio Beltram
Scuola Normale Superiore and INFM, Piazza dei Cavalieri 7, I-56126 Pisa, Italy

Silvia Rubini, Roberta Lantier,[a] and Alfonso Franciosi
Laboratorio Nazionale TASC-INFM, I-34012 Trieste, Italy

Claudio Vinegoni[b] and Lorenzo Pavesi
INFM and Dipartimento di Fisica, Università di Trento, I-38050 Povo (TN), Italy

(Received 30 October 1998; accepted for publication 9 February 1999)

Room-temperature resonant second harmonic generation is demonstrated in a ZnSe bulk microcavity with Si_3N_4/SiO_2 Bragg reflectors. The resonance occurs at the second harmonic wavelength in the blue-green spectral region and yields an enhancement of one order of magnitude in the second harmonic process. Tunability of the resonant effect between 480 and 500 nm is achieved by varying the angle of incidence. © *1999 American Institute of Physics.* [S0003-6951(99)01514-4]

Frequency-doubling devices are presently attracting a great amount of interest because they allow generation of coherent emission at wavelengths not directly accessible to available laser diodes. Such devices have been successfully implemented using nonlinear crystals such as MgO-doped $LiNbO_3$.[1] High parallel integration and the need for compact micron-sized devices, however, may require the use of semiconductor heterostructures as nonlinear crystals. Indeed, semiconductors with a zinc-blende structure exhibit strong second-order susceptibilities. In addition, the possibility to control their structures down to the atomic scale makes it possible to taylor their nonlinear response with great accuracy.[2,3] In particular, for coherent blue-green light generation, the semiconductor-based second-harmonic generation (SHG) stage can be integrated with available lasers operating in the infrared spectral region.[4] To this end, various techniques have been applied, mostly in GaAs-based materials, in order to increase the efficiency of the second-order process. Most of them rely on the design of specific asymmetric quantum well sequences[5] to achieve a quasi-phase-matched condition or on the insertion of bulk semiconductors in an optical cavity.[4,6,7]

Wide-gap II–VI semiconductors with zinc-blende structures display large second-order susceptibilities[8] and can be grown epitaxially on III–V substrates. Such materials may make possible further improvements in the SHG process. They yield frequency doubling in the blue-green spectral region without absorption of the fundamental wave in the near infrared. This excitation scheme was recently exploited by some of the authors in $Zn_{1-x}Cd_xSe/ZnSe$ asymmetric coupled quantum wells[9] where interband SHG at 470 nm was demonstrated. By appropriate design of the heterostructure profile, marked low-temperature resonant excitonic contribution to the SHG was obtained yielding a threefold enhancement with respect to the bulk ZnSe values.

In this letter, we take a different approach to enhance the nonlinear response. We demonstrate room-temperature (RT) blue-green SHG from a microcavity in which the core of the resonator is a bulk ZnSe layer and the harmonic frequency resonates with the photonic mode of the cavity. Within this scheme, frequency doubling occurs without absorption either of the fundamental or of the harmonic and yields an enhancement of one order of magnitude in the second harmonic intensity relative to the bulk. Tunability of the resonant effect between 480 and 500 nm as a function of the incident angle was also demonstrated.

Figure 1(a) shows a sketch of the bulk 2λ microcavity used in this study. The sample was grown by solid-source molecular beam epitaxy (MBE) on a Si-doped GaAs(001) substrate, utilizing a facility with interconnected MBE chambers for the growth of II–VI and III–V materials. A 0.5-μm-thick *n*-type GaAs(001) buffer epitaxial layer was first grown at temperature of $T=580\,^{\circ}C$, followed by the growth of the ZnSe (nominal thickness 392 nm) at $T=290\,^{\circ}C$ and with a Zn/Se beam pressure ratio (BPR)≈ 1. The good quality of the ZnSe layer was confirmed by a photoluminescence analysis of the low-temperature exciton-polariton emission peak (not shown) that showed a full-width at half-maximum (FWHM) of $\approx$3 meV. In order to perform the SHG experiment in a transmission geometry [Fig. 1(a)], the sample substrate was mechanically thinned down to about 200 μm and circular areas of the GaAs substrate about 200 μm in diameter were selectively removed using standard photolithographic and wet-etching techniques. Then two cavity mirrors were deposited. They were constituted by distributed Bragg reflectors, composed of 10 pairs of Si_3N_4/SiO_2 $\lambda/4$ layers with nominal thickness of 59.8 and 79 nm, respectively.[10] The deposition of the mirror layers was performed by plasma-enhanced chemical vapor deposition at a substrate temperature of $T=280\,^{\circ}C$. Reflection and transmission spectra were recorded at RT using a 100 W Xenon lamp and a double spectrometer with a 0.004 nm resolution.

Second-harmonic measurements were performed at RT using a frequency-doubled, mode-locked Ti:sapphire laser operating in a range variable between 880 and 1010 nm. Repetition rate was 82 MHz with pulse duration of 2.1 ps. The time-averaged excitation power for all measurements, except for those performed as a function of power, was 60 mW at 82 MHz. This resulted in a peak power of $\approx$34 W

[a]Present address: Institut fuer Schicht- und Ionentechnik Forschungszentrum Juelich GmbH Postfach 1913, D-52428 Juelich, Germany.
[b]Present address: University of Pittsburgh, Dept. of Physics, 100 Allen Hall, 3941 Ohara Street, Pittsburgh, PA 15260.

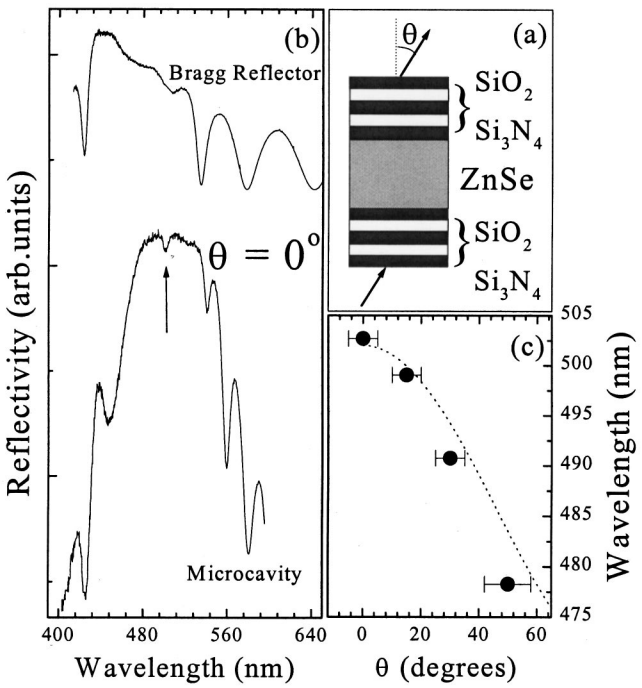

FIG. 1. (a) Sketch of the ZnSe microcavity and of the transmission geometry adopted in the experiment. The two Bragg reflectors are composed by ten pairs of Si_3N_4 and SiO_2. (b) Room-temperature normal-incidence reflectivity spectra of a Bragg reflector (top solid line) and of the ZnSe microcavity (bottom solid line). Vertical solid line and arrow indicates the cavity mode. (c) Dependence of the Fabry–Perot mode wavelength on the incident angle θ. The dotted line through the data is a fit to the equation $\lambda(\theta) = \lambda_0\sqrt{1-n^{-2}\sin^2(\theta)}$ where $n=2.82$ is the ZnSe index of refraction and $\lambda_0 = 502$ nm.

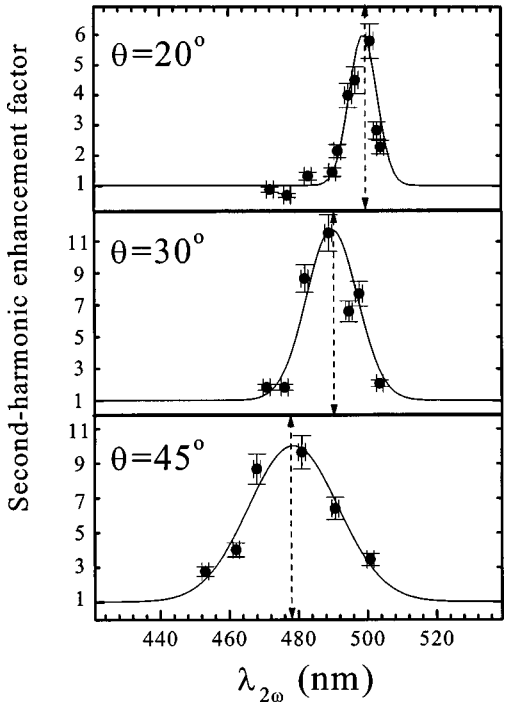

FIG. 2. Room-temperature second-harmonic (SH) enhancement factor with respect to the off-resonance response (solid circles) as a function of the SH wavelength at three different angles of incidence. The incident power was ≈60 mW. Vertical dashed lines and arrows indicate the positions of the Fabry–Perot resonance as derived from transmission spectra. Solid lines represent Gaussian fit to the experimental points.

and an energy per pulse of approximately 0.7 nJ. The laser spot on the sample had a diameter of ≈60 μm, yielding a peak excitation intensity of ≈900 kW/cm^2. The radiation emitted from the microcavity was dispersed by a 0.25 m spectrometer using a 150 grooves/mm grating and slit width of 40 μm. A band-pass filter was used to prevent the laser light from entering the spectrometer. Detection was performed with a streak-camera operating in photon counting mode.

Figure 1(b) shows the reflectivity spectra of the microcavity for an angle of incidence $\theta = 0°$ at RT and of a Bragg reflector deposited on a Si substrate. At the center of the stop band, the mirror reflectivity is around 0.9. At $\theta = 0°$, the microcavity Fabry–Perot (FP) mode (vertical solid line and arrow) is centered at about $\lambda_0 = 502$ nm with FWHM≈5 nm. Assuming that the ZnSe index of refraction is $n = 2.82$[11] at this wavelength, the position of the FP mode correlates with a thickness of the ZnSe active layer of 360 nm in good agreement with the nominal value. Figure 1(c) shows the θ dependence of the FP mode wavelength. The FP mode shifts towards lower wavelength with increasing θ according to $\lambda(\theta) = \lambda_0\sqrt{1-n^{-2}\sin^2(\theta)}$, [dotted line in Fig. 1(c)] and increases in width (from 5 to ≈15 nm). The latter effect is related to the degradation of the optical quality of the microcavity when the optical path inside the core cavity layer and mirror layers is modified from the ideal $\theta = 0°$ case. Marginal deviation from the experimental points shown in Fig. 1(c) indicates possible effects related to the angle dependence of the field penetration depth in the dielectric mirror.

The resonant condition with the FP mode and the resulting SHG tunability are demonstrated in Fig. 2. The RT SHG intensities normalized to the off-resonant SHG (solid circles) as a function of second-harmonic wavelength is shown at incidence angles $\theta = 20°$, 30°, and 45°, for an incident power of 60 mW. The observed dependence is dominated by a resonant enhancement which occurs when the emitted second-harmonic photon resonates with the cavity mode. This is clearly seen from the comparison with the observed position of the FP mode (dashed lines and vertical arrows) derived from the analysis of the corresponding transmission or reflection spectra [see Fig. 1(c)]. Again we find that the width of the resonance in Fig. 2 drastically increases for larger angles as observed for the FP modes in transmission and reflection spectra.

In order to estimate the conversion efficiency of the process, we first calculated the SH power $P_{2\omega}^{\text{bulk}}$ emitted from a bulk ZnSe layer having the same thickness of the active layer of the microcavity and at 60 mW of incident power. Given that the SH susceptibility at 500 nm is $\chi^{(2)} \approx 4 \times 10^{-11}$ m/V,[8] we found $P_{2\omega}^{\text{bulk}} = 40$ fW. From the general theory[12] it follows that if the phase mismatch is negligible (i.e., the coherence length l_c for the SHG process is much longer than the cavity layer thickness L_{cav}) the cavity confinement of harmonic light yields an enhancement with respect to the bulk of the order of $1/(1-R)$ in the SHG emitted power, where R is the mirror reflectivity at the harmonic frequency. This condition is well verified in our case where $l_c = 1500$ nm and $L_{\text{cav}} = 360$ nm. With $R \approx 0.9$, we estimate $P_{2\omega}^{\text{cavity}} \approx 10 \times P_{2\omega}^{\text{bulk}} \approx 0.4$ pW.

The ratio of the emitted power in the in-resonance case and the off-resonance case is theoretically given by $1/(1-R)^2$; as it can be observed in Fig. 2, the experimental

results are smaller than the theoretical prediction of about 100. This is attributed to the degraded optical quality of the cavity at a finite $\theta \neq 0$ incidence angle and to the difficulty of the determination of the very weak off-resonant SH emitted power.

Finally, the analysis of the second harmonic emission intensity at 471 nm (incident beam at 942 nm) as a function of incident intensity for $\theta = 45°$ is displayed in Fig. 2 showing the expected quadratic dependence of the SHG process. To verify the polarization selection rule we varied the incident beam polarization from $\phi = 0°$ (p polarization in the plane of incidence) to 90° (s polarization normal to the plane of incidence). The results are displayed in the inset of Fig. 2 together with the results of the best fit (dotted line) to the theoretical curve $I_2 \propto |\chi^{(2)}_{xyz}|^2 |E_z|^2 |E_y|^2$, where $\chi^{(2)}_{xyz}$ is the second-order susceptibility involved in the SHG, x, y, and z are the crystallographic axis (z is the growth direction), and E_z, E_y are the z and y components of the incident electric field.

In order to gauge the contribution to the second-harmonic process coming from the ZnSe cavity layer in which light is confined, we carried out a similar analysis in a reflection geometry on a single Bragg reflector deposited on a Si substrate. In this case no detectable SHG was observed in the same experimental conditions previously adopted to obtain the results in Fig. 3 thus suggesting the predominant role played by the cavity layer in the nonlinear process.

As we have already said, the single resonance condition for the harmonic photon is expected to give a cavity enhancement of the second-harmonic power of the order of $1/(1-R)$ with respect to the bulk; an improvement of the efficiency can thus be obtained by increasing the reflectivity of the mirrors. To further increase of the SHG power, it is possible to use a microcavity in which also the fundamental frequency resonates with a cavity mode. In this case, the cavity enhancement is given by $1/(1-R)^3$. With an improved reflectivity of the order of 0.99 a six order of magnitude of enhancement of the SH power with respect to bulk is expected. In this double-resonant configuration, the emitted SH power would be of the order of tenths of μW.

In conclusion, we have reported room-temperature resonant SHG in a 2λ ZnSe bulk microcavity with dielectric mirrors. The SH light was generated in the blue-green spectral region after excitation below the half band-gap region of the ZnSe layer in order to avoid band-to-band absorption at the fundamental and harmonic frequencies. The SHG process is enhanced by one order of magnitude when the second-harmonic photon resonates with the Fabry–Perot mode of the cavity. The tunability of the cavity mode wavelength as a function of incident angle allows resonant SH emission between 480 and 500 nm. These results provide a promising framework for the implementation of frequency-doubling devices based on wide-gap II–VI semiconductors. They also show, for the first time, the selective contribution of the microcavity resonant condition with the SH photon to the SH conversion efficiency and demonstrate the use of a novel material system for the doubling in the visible. The magnitude of this effect is in quantitative agreement with calculation. We have shown that several avenues are available to further increase the SHG conversion process. These includes control of the phase of the mirror reflection coefficient, use of different geometries for the fundamental and harmonic wave propagation,[13] and realization of double resonant microcavities at both the fundamental and harmonic waves.[7]

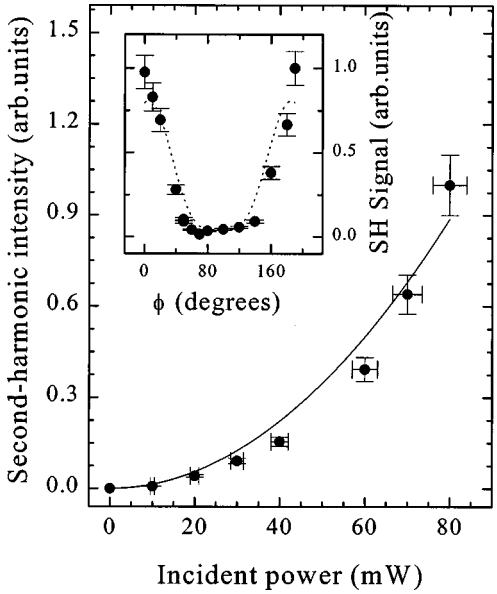

FIG. 3. Second-harmonic (SH) intensity at 471 nm as a function of the incident power at 942 nm with incident angle $\theta = 45°$. Solid line corresponds to a quadratic fit to the experimental points. The inset shows the dependence of the SH signal on the incident polarization angle ϕ. $\phi = 0°$ corresponds to the pump beam linearly polarized in the plane of incidence (p polarization). Dotted line represents the best fit with the equation $I_2 = \alpha |\chi^{(2)}_{xyz}|^2 |E_z|^2 |E_y|^2$, where $\chi^{(2)}_{xyz}$ is the second-order susceptibility involved in the SH process, x, y, and z are the crystallographic axis (z is the growth direction), and E_z, E_y are the z and y components of the incident electric field. The fit corresponds to an azimuthal angle $\psi = 80°$ between the plane of incidence and the y crystallographic axis.

The authors acknowledge Giuseppe La Rocca for fruitful discussions. The work at TASC-INFM was supported in part by the Consiglio Nazionale delle Ricerche of Italy under the MADESS project. The authors thank the entire staff of the Microtechnology Laboratory at the University of Minnesota for their expert assistance.

[1] K. Fiedler, S. Schiller, R. Paschotta, P. Kurz, and J. Mlynek, Opt. Lett. **18**, 1786 (1993).
[2] C. Sirtori, F. Capasso, D. L. Sivco, S. N. G. Chu, and A. Y. Cho, Appl. Phys. Lett. **59**, 2301 (1991).
[3] E. Rosencher, A. Fiore, B. Vinter, V. Berger, Ph. Bois, and J. Nagle, Science **271**, 168 (1996).
[4] N. Yamada, Y. Kaneko, S. Nakagawa, D. E. Mars, T. Takeuchi, and N. Mikoshiba, Appl. Phys. Lett. **68**, 1895 (1996).
[5] S. Janz, F. Chatenoud, and R. Normandin, Opt. Lett. **19**, 622 (1994).
[6] P. A. Ramos and E. Towe, Appl. Phys. Lett. **69**, 3321 (1996).
[7] C. Simonneau, J. P. Debray, J. C. Harmand, P. Vidakovic, D. J. Lovering, and J. A. Levenson, Opt. Lett. **22**, 1775 (1997).
[8] H. P. Wagner, Phys. Status Solidi B **187**, 363 (1995).
[9] V. Pellegrini, A. Parlangeli, M. Börger, R. D. Atanasov, F. Beltram, L. Vanzetti, and A. Franciosi, Phys. Rev. B **52**, R5527 (1995).
[10] The indeces of refraction for the Si_3N_4 and SiO_2 layers fabricated here were $n_1 = 1.92$ and $n_2 = 1.455$, respectively, as derived from ellipsometry measurements.
[11] Landolt-Börnstein, *Numerical Data and Functional Relationship in Science and Technology*, edited by O. Madelung (Springer, Berlin, 1982), New Series Group III, Vol. 17.
[12] V. Berger, J. Opt. Soc. Am. B **14**, 1351 (1997).
[13] Y. J. Ding, J. B. Khurgin, and S. J. Lee, J. Opt. Soc. Am. B **12**, 1586 (1995).